Original Research

A novel fluorescent traceable carbon quantum dots with selective antibacterial activity against *Porphyromonas gingivalis*

Jie Wang[1,2*], Yan Wang[1*], Hang Zhang[1], Weiwen Zhu[1] and Laikui Liu[1,3]

[1]Jiangsu Key Laboratory of Oral Diseases, Jiangsu Province Engineering Research Center of Stomatological Translational Medicine, Nanjing Medical University, Nanjing 210029, China; [2]Department of General of Dentistry, The Affiliated Stomatological Hospital of Nanjing Medical University, Nanjing 210029, China; [3]Department of Basic Science of Stomatology, The Affiliated Stomatological Hospital of Nanjing Medical University, Nanjing 210029, China
*These authors contributed equally to this paper.
Corresponding author: Laikui Liu. Email: my_yunkong@njmu.edu.cn

Impact Statement

Porphyromonas gingivalis is closely related to many diseases. Antibiotics can effectively kill *P. gingivalis*, but overuse is prone to drug resistance. The development of nanomedicine, carbon quantum dots (CDs) are a novel and fluorescent traceable nanoscale material, possessing antibacterial potential. In this study, we developed and screened CDs of specific molecular weight, prepared for the first time using ornidazole as raw material and microwave radiation method. The fluorescence property and inhibitory effect of CDs on *P. gingivalis* are also emphatically discussed. To sum up, it illustrated that our newly synthesized ornidazole CDs had a selective antibacterial effect on *P. gingivalis*, which provided a new strategy for the treatment of diseases related to *P. gingivalis* and further promoted the development of nano biomedicine.

Abstract

Antibiotics can kill bacteria, but their continued use can easily lead to drug resistance, particularly the main pathogenic bacteria of periodontitis, *Porphyromonas gingivalis*. However, to avoid drug resistance, carbon quantum dots (CDs) have great potential as a bioactive material in antimicrobial therapy. Herein, we use ornidazole as raw material to prepare CDs of different sizes by microwave irradiation and screen CDs with fluorescence and bacteriostatic properties. The inhibition experiments and live/dead assays of *P. gingivalis* exhibited outstanding antibacterial effects. This research aimed to develop nano-level antibacterial active materials that also have fluorescence traceability. This study offers a different method for the development of multifunctional CDs, provides valuable strategies for the treatment of diseases associated with *P. gingivalis*, and predicts great application prospects in the field of biomedicine.

Keywords: Carbon quantum dots, traceable, antibacterial activity, *Porphyromonas gingivalis*

***Experimental Biology and Medicine* 2023; 248: 2227–2236. DOI: 10.1177/15353702231211867**

Introduction

Periodontitis is a common and frequently-occurring disease in the oral cavity, affecting more than 90% of patients with dental conditions.[1] Periodontal pathogens are important factor leading to periodontitis, and Gram-negative anaerobe such as *Porphyromonas gingivalis* is the main pathogenic bacteria of periodontitis.[2] *P. gingivalis* is very common in the oral cavity of adults, and oral diseases related to *P. gingivalis* become more serious with age.[3] Abnormally increased numbers of *P. gingivalis* cause oral microbial flora dysbiosis and microenvironmental dysbiosis. In such a situation, the bacterium is highly pathogenic and destroys the periodontal tissue and sometimes even enters the blood circulation system, leading to some systemic diseases and complications, such as diabetes, premature birth, hypertension, cardiovascular disease, and pneumonia.[4] Meanwhile, some studies have shown that, in patients with oral squamous cell carcinoma, *P. gingivalis* is significantly higher than in normal people, indicating that *P. gingivalis* may be involved in the occurrence and development of squamous cells carcinoma.[5] *P. gingivalis* is also a risk factor for pancreatic cancer and colorectal cancer,[6] and higher levels of *P. gingivalis* have also been detected in the oral cavity of patients with Alzheimer's disease.[7] Thus, *P. gingivalis* is closely related to many diseases besides periodontitis, and therefore highlights the significance in the treatment and prognosis of these diseases, rendering the eradication of *P. gingivalis* vital in treating periodontitis or other related diseases.

Currently, clinical practice entails the use of antibiotics to kill *P. gingivalis*.[8] However, in addition to good bacteriostatic

effects, antibiotics are prone to developing resistance, hence greatly limiting their long-term use.[9,10] In addition, the effective performance time of most antibiotics is limited in clinical practice. Bacteria can produce biofilms, and those located under the biofilms can evade the action of antibiotics and host defense mechanisms, leading to drug action failure and bacterial resistance. At this point, increasing the drug dose can only further enhance bacterial resistance. The development of a bioactive material that can effectively cause bacteriostasis is becoming a huge challenge. Therefore, we strive to find a new way to avoid the challenge of antibiotic resistance during the inhibition of bacterial growth.

In recent years, nanomedicine has developed exponentially, and nanomaterials such as antibacterial peptides and inorganic nanoparticles have been developed as antibacterial drugs for the treatment of infectious diseases caused by bacteria.[11] Carbon quantum dots (CDs) exhibit excellent antibacterial properties due to their small size. As a new type of nanomaterial, its preparation is simple and easily modifiable, and it has many unique characteristics, such as excellent low toxicity, biocompatibility, high photostability, optical properties, good water solubility, and cell permeability.[12,13] CDs are carbon-based fluorescent nanomaterials. In recent years, CDs have been widely considered to have great application prospects due to their unique adjustable photoluminescence (PL), good biocompatibility, low toxicity, and other biomedical characteristics.[14] Several approaches are used for the synthesis of CDs, including microwave radiation, chemical ablation of hydrothermal treatment, laser ablation, and electrochemical carbonization;[15] among these, the microwave radiation method is a complete, green, and simple synthesis method.[16] CDs are rich in carbon and can be prepared from a variety of raw materials, such as drugs, fruits, food, and hair.[17–20] According to some scholars, carbon quantum dots prepared from spermidine or quaternary ammonium salts have certain antibacterial ability against Gram-positive and Gram-negative bacteria and their carbonization enhances their antibacterial properties.[21,22] CDs made from gentamicin sulfate,[23] aminoguanidine,[24] and citrus limetta,[25] as sources also achieved obvious antibacterial effects. Novel medicine that selectively targets pathogenic bacteria provides a viable alternative to the overuse of broad-spectrum antibiotics. Some scholars used metronidazole as a source to prepare carbon nanoparticles, which have selective antibacterial activity, especially against anaerobes.[13] As the advanced version of metronidazole, ornidazole is also highly effective against Gram-negative anaerobic bacteria. Therefore, we speculate that the nanoscale size of ornidazole CDs can penetrate the bacterial membrane, thereby achieving the effect of splitting bacteria.

In this study, we successfully prepared different sizes of ornidazole CDs for the first-time, using the microwave radiation method (Figure 1), and selected 1-10K CDs with good fluorescence and strong antibacterial properties. The 1-10K CDs were strongly antibacterial against *P. gingivalis*, but not *Streptococcus mutans*. Thus, the main purpose of this study was to develop a novel fluorescent traceable and selectively bacteriostatic CDs, to provide a new strategy for the diagnosis and treatment of *P. gingivalis*-related diseases, and to provide a new perspective for targeted treatment using nanomedicine.

Materials and methods

Synthesis of carbon quantum dots

CDs were explored through the microwave irradiation approach following previous reports.[26] Briefly, 2.19 g ornidazole (10 mmol) (Shanghai Aladdin Reagent Co. Ltd) was precisely weighed into a beaker with 250 mL water and add 5 mL anhydrous ethanol to fully dissolve ornidazole. The beaker was heated in a domestic microwave oven (placed in a fume hood) at 700 W (full power) for 3 min to obtain a thick brown and black oily/granular mixture. The products were dispersed in 30 mL purified water and placed in an ultrasonic water bath for 20 min. Afterwards, graded centrifugation ultrafiltration was carried out by millebo 1K MWCO, 10K MWCO, and 30K MWCO ultrafiltration tubes at 5000 r/min. First, we used 1K MWCO ultrafiltration tubes at 5000 r/min for filtration, leaving behind nanoparticles larger than 1K. Then, 10K MWCO ultrafiltration tubes were used for filtration, and the filtered material was recycled to form 1-10K CDs. The remaining substances larger than 10K were filtered using 30K MWCO ultrafiltration tubes, and the filtered substances were also recycled to form 10-30K CDs. Then, the volume of the graded recycled filtrate was subjected to dialysis and resized to 30 mL to obtain solutions of ornidazole quantum dot with a range of different molecular weights. The obtained liquid was freeze-dried overnight to form solid CDs for further characterization.

Characterization of carbon quantum dots

The CDs and their energy dispersive spectroscopy (EDS) patterns were also acquired by high-resolution transmission electron microscopy (HRTEM) (JEM-2100 F; Japan). The size distribution of nanoparticles was examined using the Zetasizer Nano ZS instrument (Malvern, UK). The fluorescence emission spectra of CDs were analyzed on the Hitachi FluoroMax-4 fluorescence spectrometer. Obtaining UV-Vis absorption spectra using the Shimadzu 3100 UV-Vis spectrophotometer. The Fourier transform infrared (FTIR) spectra of CDs were recorded by Nicolet 200 Fourier transform infrared spectrometer (Thermo Nicolet, USA). Fluorescent images were captured using Olympus IX83 under ultraviolet light.

Cell cytotoxicity of carbon quantum dots

Human periodontal ligament stem cells (hPDLSCs) were extracted from human periodontal ligament for the estimation of cytotoxicity of CDs Using the Cell Counting Kit-8 (CCK8). Briefly, hPDLSCs were inoculated (3×10^3/well) to a 96-well plate and incubated at 37°C and 5% CO_2 for 1 day before co-culturing with nanoparticles; then, cells were exposed to various concentrations of CDs for another 1, 3, 5, 7, and 9 days. Thereafter, 100 μL 10% CCK8 was added to each well and incubated in the incubator at the specified time. The optical density (OD) value was determined at 450 nm using a microplate reader. The test result was represented as the mean of at least three replicates. The calculation of cell viability was as follows:

$$\text{Cell viability} = \text{ODexperiment}/\ \text{ODControl} \times 100\%$$

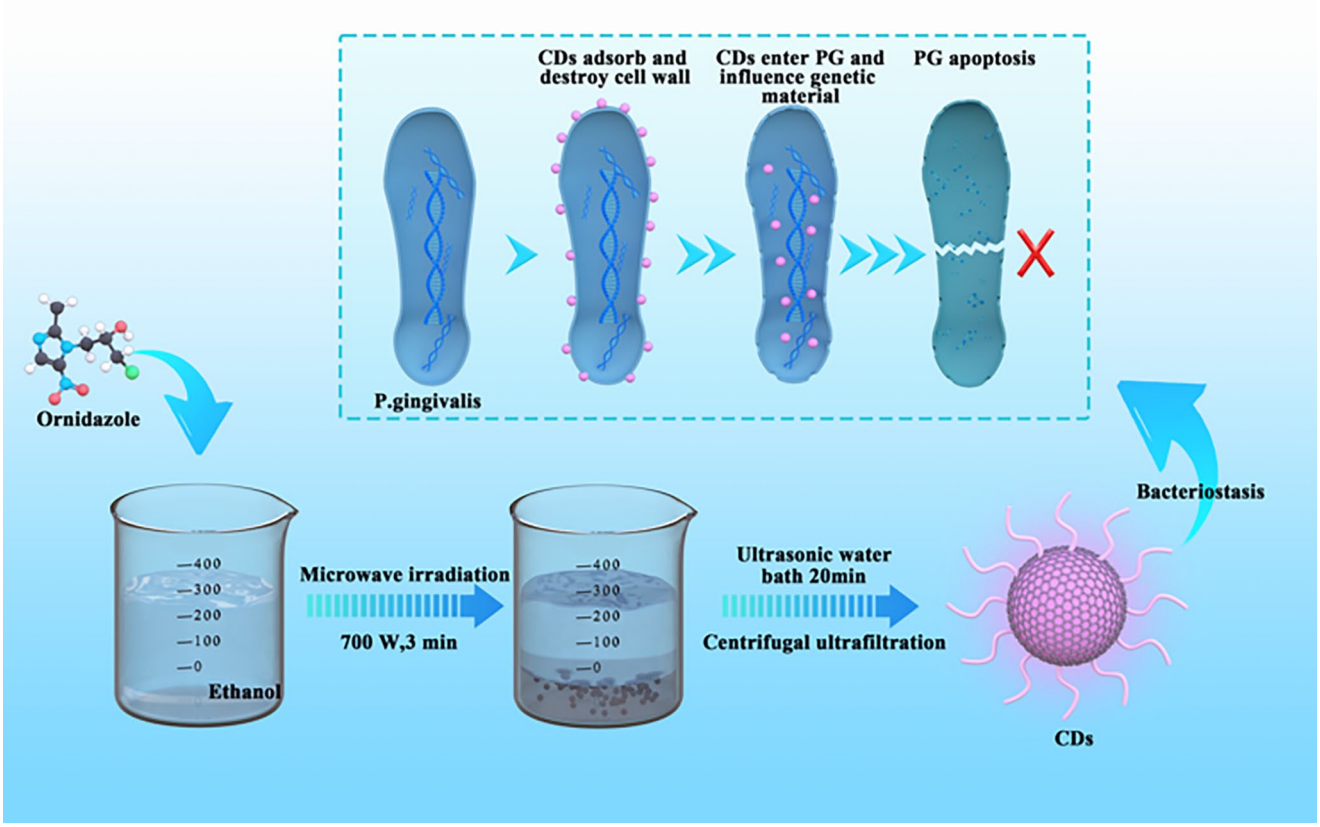

Figure 1. Schematic of synthesis and specific antibacterial activity of fluorescent carbon quantum dots.

Cellular imaging

Sterile glass slides were placed into a 24-well plate, then hPDLSCs (1×10^4/well) were grown on the glass slide with 0.1 mL of 100 μg/mL CDs. After 24 h of cultivation at 37°C in 5% CO_2, the glass slides were washed thrice with Dulbecco's phosphate buffered saline, fixed with 4% paraformaldehyde for 0.5 h, penetrated with 0.25% Triton X-100/PBS for 5 min, and finally stained with 4′,6-diamidino-2-phenylindole at room temperature in the dark for 10 min. Cell fluorescence of stained of CDs was captured by fluorescence microscopy (DM2000, Leica, Germany).

Antibacterial activity test

P. gingivalis (ATCC 33277) was obtained from Shanghai Bioresource Collection Center (Shanghai, China) and *S. mutans* (UA159) was obtained from Yiwei Biotech (Qingdao, China). *P. gingivalis* was cultivated on brain heart infusion (BHI) solid medium under anaerobic conditions (37°C, 5% CO_2, 85% N_2, 10% H_2). *P. gingivalis* was harvested in its exponential growth phase and resuspended in a BHI liquid medium for later experiments, which were the same procedure for *S. mutans*.

The antibacterial efficacy was evaluated using the inhibition zone assays as an intuitive method. Briefly, 100 μL *P. gingivalis* (5×10^8 CFU/ mL) was evenly inoculated onto a solid culture medium and kept in an anaerobic incubator (37°C, atmosphere of 85% N_2, 10% H_2, 5% CO_2) for 1 h. During the cultivation process, circular sterile filter papers of 10 mm diameter were completely immersed in the nanomaterial solution for 1 h. The treated filter paper sheets were placed into a solid medium containing the bacteria and incubated for 72 h. The size of the suppression zone was finally recorded and measured by a charge-coupled device camera. The experiments for *S. mutans* were also conducted as the above.

The spread plate method was employed as another common measure of antibacterial effect. A 100 μL *P. gingivalis* (5×10^8 CFU/ mL) suspension was incubated with 100 μL of liquid material for 24 h. Then, 100 μL of the mixture was moved and spread on the solid medium. The remaining 100 μL mixture was transferred into a test tube containing 900 μL of sterile water and mixed well to form a 10^{-1} dilution. From the 10^{-1} dilution, 100 μL of liquid was removed and added to a test tube containing 900 μL of sterile water and mixed to get a 10^{-2} dilution. This 10^{-2} dilution was added drop-wise on the agar plate and spread evenly on the plate with an L-shaped coating rod. The smeared plate was placed flat on the table for 20~30 min and then reversed and incubated in an anaerobic box. The blank control group had bacterial suspension + BHI used, and the bacterial growth on the plate was observed 7 days later.

The live/dead analysis was also conducted on the morphology and activity of the captured bacteria using the LIVE/DEAD™ BacLight™ Bacterial Activity kit.

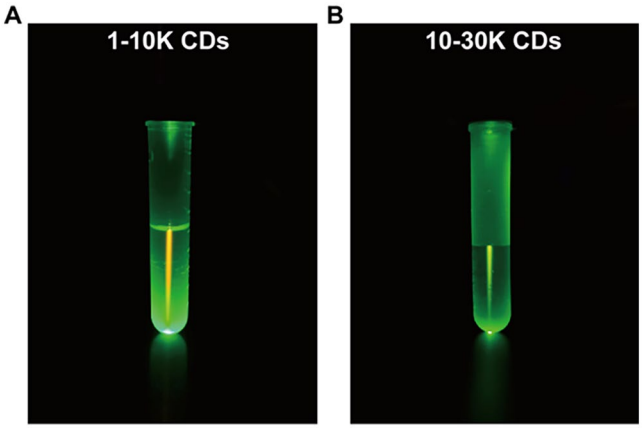

Figure 2. Fluorescent appearance of CDs: (A) 1-10K CDs and (B) 10-30K CDs. (K refers to relative molecular weight).

Statistical analysis

For data analyses, SPSS version 22 (SPSS, Chicago, IL, USA) was used. All experimental data were presented as mean ± standard deviation (mean ± SD). One-way analysis of variance and the least significant difference test were performed at $P = 0.05$ after testing the normality. All quantitative data were represented by the mean of at least three replicates.

Results

Characterization of carbon quantum dots with different sizes

Two different sizes of carbon quantum dots, 1-10K CDs and 10-30K CDs (K refers to relative molecular weight), were synthesized using ornidazole as raw material by microwave irradiation. Compared with the 10-30K CDs, the 1-10K CDs had an obvious green-red fluorescence effect (Figure 2(A) and (B)). Figure 3(A) shows the transmission electron microscopy (TEM) of ornidazole raw material. The high-resolution transmission electron microscopy (HRTEM) images exhibited mostly spherical CDs with uniform size and outstanding dispersibility, indicating their successful preparation (Figure 3(B) and (C)). The EDS spectra of ornidazole and CDs (Figure 3(A) to (C)) indicated that the 1-10K CDs consisted mainly of carbon (C; 94.62%), nitrogen (N; 0.51%), and oxygen (O; 4.87%). The 10-30K CDs mainly consisted of carbon (C; 95.47%), nitrogen (N; 0.29%), and oxygen (O; 4.24%). In contrast, ornidazole mainly comprised carbon (39.81%), N (31.93%), oxygen (21.80%), and chlorine (6.46%). The dynamic light scattering (DLS) of CDs (Figure 3(D) and (E)) indicated that the CDs were predominant of about 19 and 34 nm diameters, respectively. The bands of FTIR spectra at 3120 and 1510 cm^{-1} stand for the typical –OH and –C = C groups of the ornidazole, respectively (Supplemental Figure 1). Particularly, the appearance of low-intensity absorption bands at 1608 cm^{-1} corresponds to the asymmetric vibrations of the NO_2 group. The FTIR spectrum results of the CDs also showed that some original functional groups in 1-10K CDs still remained under high pressure and high temperature (Supplemental Figure 1). Figure 4 illustrated the UV-Vis spectra of 1-10K CDs, 10-30K CDs, and ornidazole; the prodrug ornidazole displayed three broad absorption peaks at 199, 231, and 321 nm, attributed to (–OH), π–π* (C = N), and n–π* (C–N-C), respectively, but the nano CDs showed only two peaks at 200 and 316 nm, which could be attributed to (–OH) and n–π* (C–N-C). The photoluminescent properties of CDs were examined at excitation wavelengths from 318 to 500 nm, and the results are exhibited in Figure 5(A) and (B). The 1-10K CDs, at the excitation wavelength of 400 nm and the emission wavelength of 519 nm, exhibited an outstanding emission intensity.

According to the inset image in Figure 5(A), the 1-10K CDs displayed green–red fluorescence at 519 nm and had no regularity of wavelength and no obvious fluorescence (Figure 5(B)).

Biocompatibility of carbon quantum dots

Low toxicity and good biocompatibility of the nanomaterials are vital indicators of their biomedical applications. Therefore, we first examined the cytotoxicity of 1-10K CDs and 10-30K CDs via the CCK8 assay. The hPDLSCs were treated with various concentrations of CDs for biocompatibility assays. Figure 6(A) shows that when the concentration of 1-10K CDs was within 200 μg/mL, there was no significant cytotoxicity, and the cell proliferation state was optimal at 40 μg/mL. The results of 10-30K CDs was similar with 1-10K CDs (Figure 6(B)).

Carbon quantum dots mediated cell imaging

The fluorescent images of hPDLSCs co-cultured with 1-10K CDs (the concentration is 100 μg/mL) for 1 day at 37 °C are presented in Figure 7(A). Strong red photoluminescence was detected in 1-10K CDs treated cells under the green excitation light, respectively, while 10-30K CDs (Figure 7(B)) exhibited weak red photoluminescence, which was approximately 10 times weaker than that of 1-10K CDs, and was also in accordance with the result presented in Figure 5. However, the control (without CDs) (Figure 7(C)) exhibited absolutely no photoluminescence.

Inhibition effect of carbon quantum dots on bacterial growth

Ornidazole and 1-10K CDs caused obvious bacteriostatic circles on *P. gingivalis*, while this was not so for the 10-30K CDs and control (Figure 8(A)). The radius of the inhibition zone also indicated that the 1-10K CDs had a significant antibacterial effect on *P. gingivalis* (Figure 8(B)); however, the 10-30K CDs had no effect (Figure 8(B)). Meanwhile, *P. gingivalis* incubated with 1-10K CDs (Figure 8(E)) had a significantly reduced colony number compared with the control group (bacterial + BHI) (Figure 8(C)) and 10-30K CDs group (Figure 8(D)). Figure 8(F) to (H) show the results of diluted colonies of those presented in Figure 8(C) to (E). *P. gingivalis* colonies were hardly seen in the 1-10K CDs group (Figure 8(H)), while the control (Figure 8(F)) and 10-30K CDs (Figure 8(G)) still had little colony number. The above results proved that the novel 1-10K CDs had an obvious bacteriostatic effect on *P. gingivalis*, while 10-30K CDs were not.

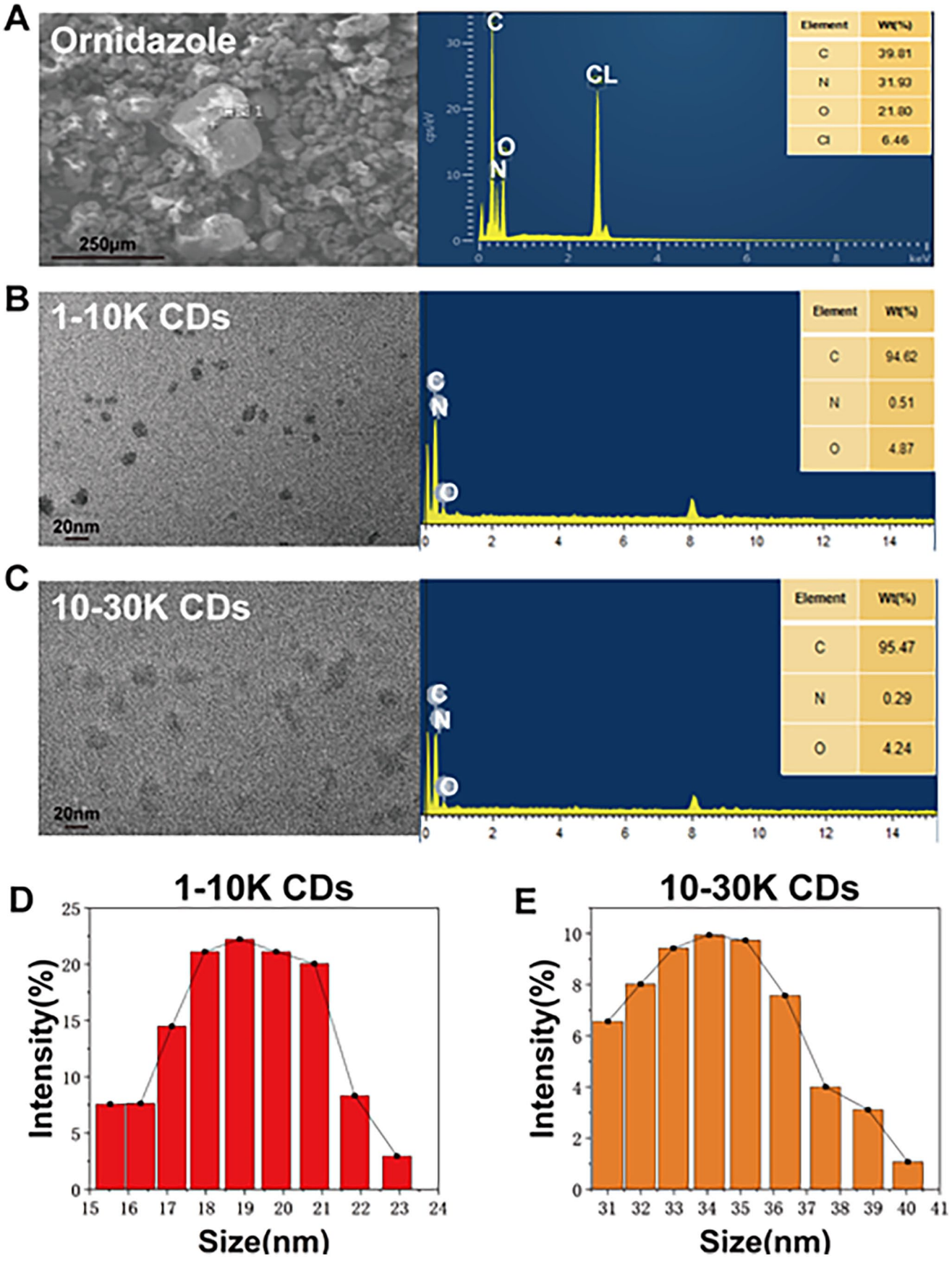

Figure 3. TEM/HRTEM and DLS of particles: (A) TEM and EDS of ornidazole, HRTEM and EDS of (B) 1-10K CDs and (C) 10-30K CDs, DLS of (D) 1-10K CDs, and (E) 10-30K CDs.

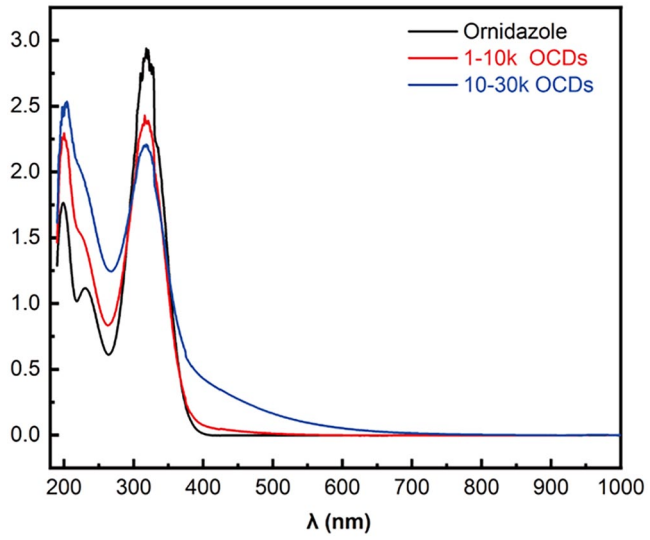

Figure 4. UV-Vis absorption spectra of ornidazole and CDs.

For *S. mutans*, no inhibitory zones were observed around filter papers treated with 1-10K CDs and 10-30K CDs (Supplemental Figure 2), indicating that both CDs had no antibacterial effect on *S. mutans*.

Typical fluorescent images of the live/dead assays for *P. gingivalis* are presented in Figure 9. Obviously, several live *P. gingivalis* were detected in the control group, but only a small number of live bacteria could be seen on the plates having *P. gingivalis* treated with 1-10K CDs or ornidazole. Moreover, a high number of dead bacteria was observed in the 1-10K CDs group. This was consistent with the previous results of the suppression zone (Figure 8). Therefore, the 1-10K CDs were chosen for further study, and all the above-mentioned results suggest that novel 1-10K CDs synthesized by ornidazole are potential antibacterial materials.

Discussion

P. gingivalis is a Gram-negative anaerobic bacterium that leads to the occurrence and development of periodontitis.[2,27] In addition, *P. gingivalis* is also potentially associated with many other systemic diseases.[5,7] It is evident that killing *P. gingivalis* is crucial for the treatment of diseases related to it. Presently, antibiotics are commonly used to eliminate *P. gingivalis* infection, but long-term use of antibiotics is prone to cause drug resistance. Hence, with the rise of nanomedicine technology, CDs, as an advanced nanomaterial, can avoid the drug resistance caused by excessive drug use and, as an advantage, utilize their nanoscale size to penetrate the bacterial cell membrane, thereby achieving antibacterial effects.

The synthesized CDs using drugs as precursors, in addition to obtaining nanoscale particles that can easily penetrate the bacterial membrane, often retain some specific sterilization groups of the original drugs, thereby exerting good antibacterial effects.[28] Ornidazole is a nitroimidazole antibiotic effective against Gram-negative and anaerobic bacteria, especially *P. gingivalis*. Therefore, ornidazole was selected as the carbon source in this study. Meanwhile, the microwave radiation method is a very simple, convenient, and green method for CDs synthesis. Therefore, the synthesis of CDs with optical properties in a simple, green, and low-cost manner is possible.

In this study, we synthesized CDs with ornidazole, especially employing a green and simple microwave irradiation method.[26,29–31] We screened two synthesized CDs of different sizes to obtain specific-sized CDs with the best fluorescence and antibacterial properties. Among these, 1-10K CDs exhibited obvious red fluorescence under green excitation light, and their microscopic morphology was generally spherical, with nearly 19 nm diameter, and uniformly dispersed. However, the 10-30K CDs exhibited significantly weaker fluorescence performance, presenting a spherical shape with a diameter of about 34 nm. The elemental composition indicated that the carbon content increased after the reaction, and carbon polymerization occurred in CDs, revealing that the carbon dots were successfully prepared. The prepared nanoparticles were evenly dispersed in water and had good water solubility. The main characteristic functional groups of CDs, such as (–OH) and n–π^* (C–N-C), were successfully identified. According to reports, anaerobic bacteria could revert the nitro group of nitroimidazole to hydroxylamine groups through electron transfer, thereby reacting with bacterial DNA and proteins, and preventing the synthesis of all nucleic acids.[13,32,33] FTIR and UV-Vis assessment exhibited a successful synthesis of CDs through the microwave irradiation approach, and they retained the special antibacterial group.[13] The 1-10K CDs exhibited excellent fluorescent property at 400 and 519 nm, the excitation wavelength and emission wavelength, while 10-30K CDs had poor fluorescence. In fact, good biocompatibility is a key factor for applications in bio-imaging and biomedicine. The above results showed good biocompatibility and low toxicity of the two types of CDs. Since CDs are likely to be absorbed by cells by endocytosis and quickly excreted from the body, they are non-toxic and have penetrating properties. This work opens a new method for exploring the mode of action on ornidazole CDs and provides valuable strategies for the diagnosis and treatment of some diseases. Thus, these CDs hold promising potential in applications in biomedicine, including bio-imaging. As shown above, CDs showed a prominent excitation-dependent photoluminescence, suggesting that changing the excitation wavelength could easily adjust the emission wavelength, thus aiding in multicolor biological imaging. Subsequently, CDs co-cultured with hPDLSCs, and the cell imaging ability was observed. CDs were found to gather and contact around some cells, indicating some interaction among them. These results demonstrated good biocompatibility of the 1-10K CDs, and subsequently, fluorescence traceability.

As a commonly used antibacterial drug, ornidazole is especially effective against Gram-negative and anaerobic bacteria. However, the overuse of drugs could easily result in bacterial resistance, and it was easy to produce biological toxicity, limiting its clinical applications.[34] We determined the specific antibacterial effects of novel ornidazole CDs of different molecular weights on the growth and reproduction of different bacteria, and thus avoid the occurrence of antibiotic resistance. Thus, the tests to determine the inhibitory zone were conducted with CDs and *S. mutans* and *P. gingivalis*.

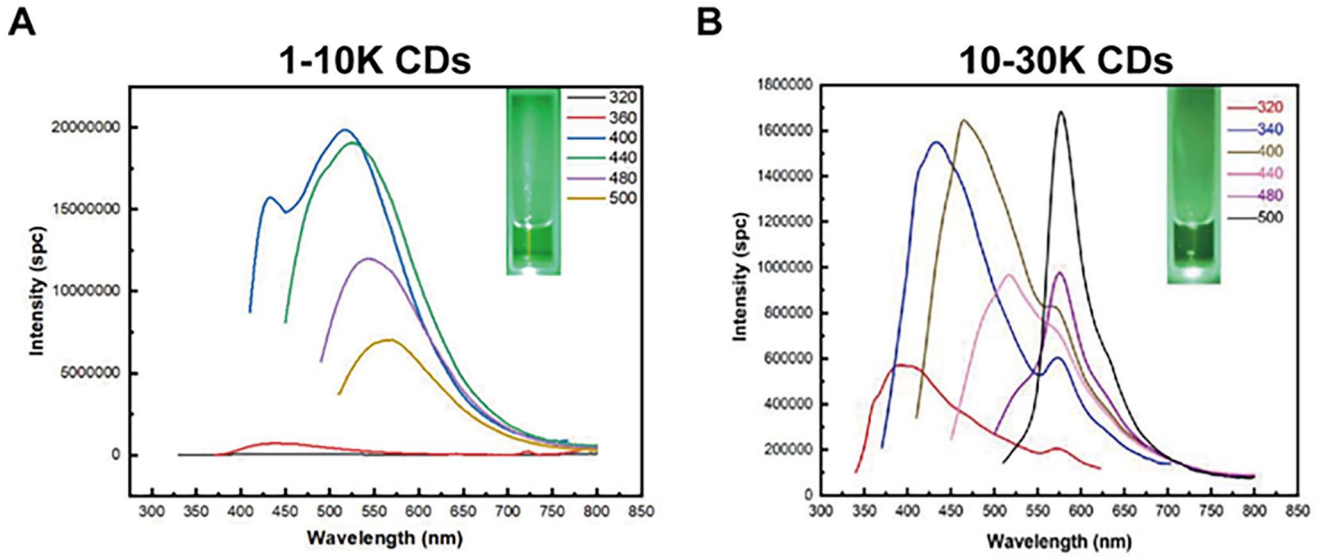

Figure 5. Photoluminescent excitation and emission spectra of CDs: (A) 1-10K CDs and (B) 10-30K CDs.

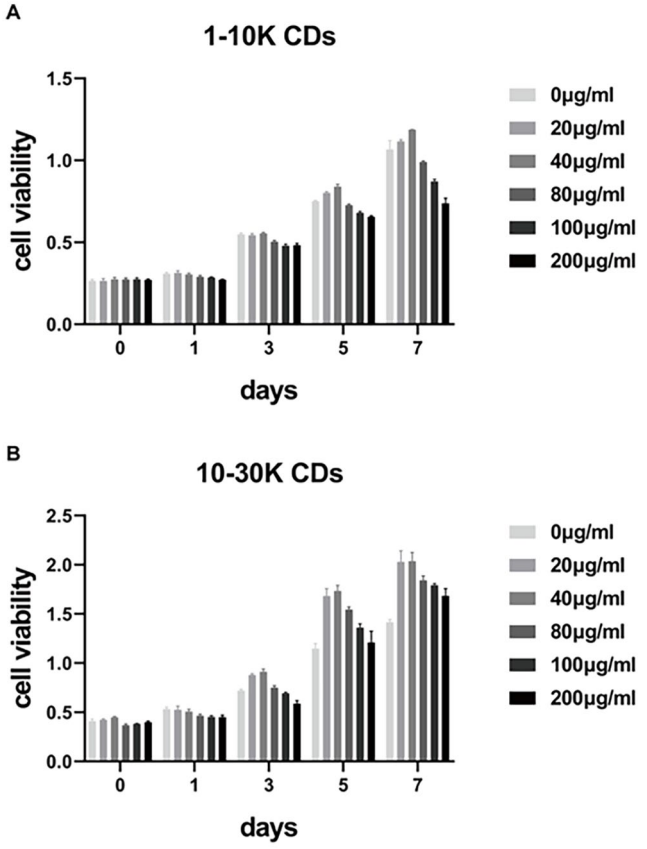

Figure 6. Cell viability of hPDLSCs after incubation with various concentrations of CDs: (A) 1-10K CDs and 10-30K CDs.

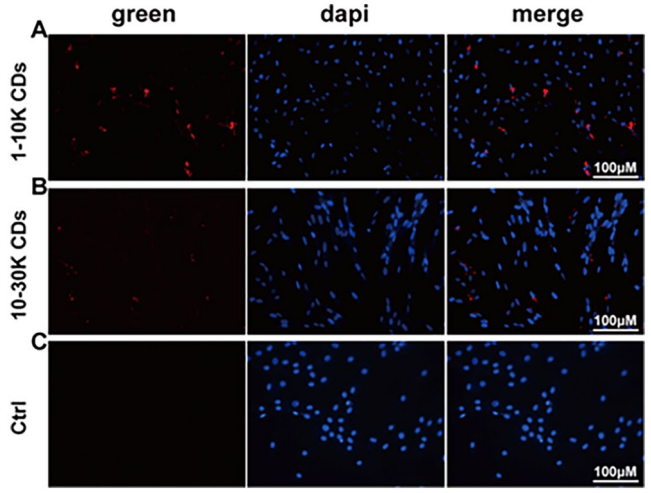

Figure 7. Fluorescence images of hPDLSCs incubated with (A) 1-10K CDs, (B) 10-30K CDs, and (C) Ctrl for 24 h (red fluorescence is CDs, blue fluorescence is dapi).

We found that 1-10K CDs exhibited an outstanding antibacterial effect on *P. gingivalis*, while the 10-30K CDs did not. The typical live/dead tests of *P. gingivalis* also validated significant antibacterial effects of 1-10K CDs. There are reports indicating that the antibacterial properties of many antibacterial agents are closely related to their size and that the molecular size of antibacterial agents is closely related to their ability to enter and destroy bacterial membranes. Bacterial membrane damage can manifest as membrane thinning and disorder. Materials with relatively small molecular weights can cause thinning of the bacterial membrane and interfere with intracellular activity, exhibiting rapid and efficient antibacterial activity. The molecular size of the material is critical, allowing the nanomaterial to just enter the bacterial cell membrane without rupturing the bacterial membrane, thus not being able to effectively kill bacteria.[35] Therefore, different molecular sizes can affect the antibacterial performance of the material. The antibacterial mechanism of CDs mentioned in existing literature mainly manifests as a nanoscale structure that can penetrate the bacterial cell membrane, thereby lysing the bacterial cell.[28] Similarly, the molecular size is also a critical factor, below which, the smaller the molecular weight, the more significant the penetration effect, and

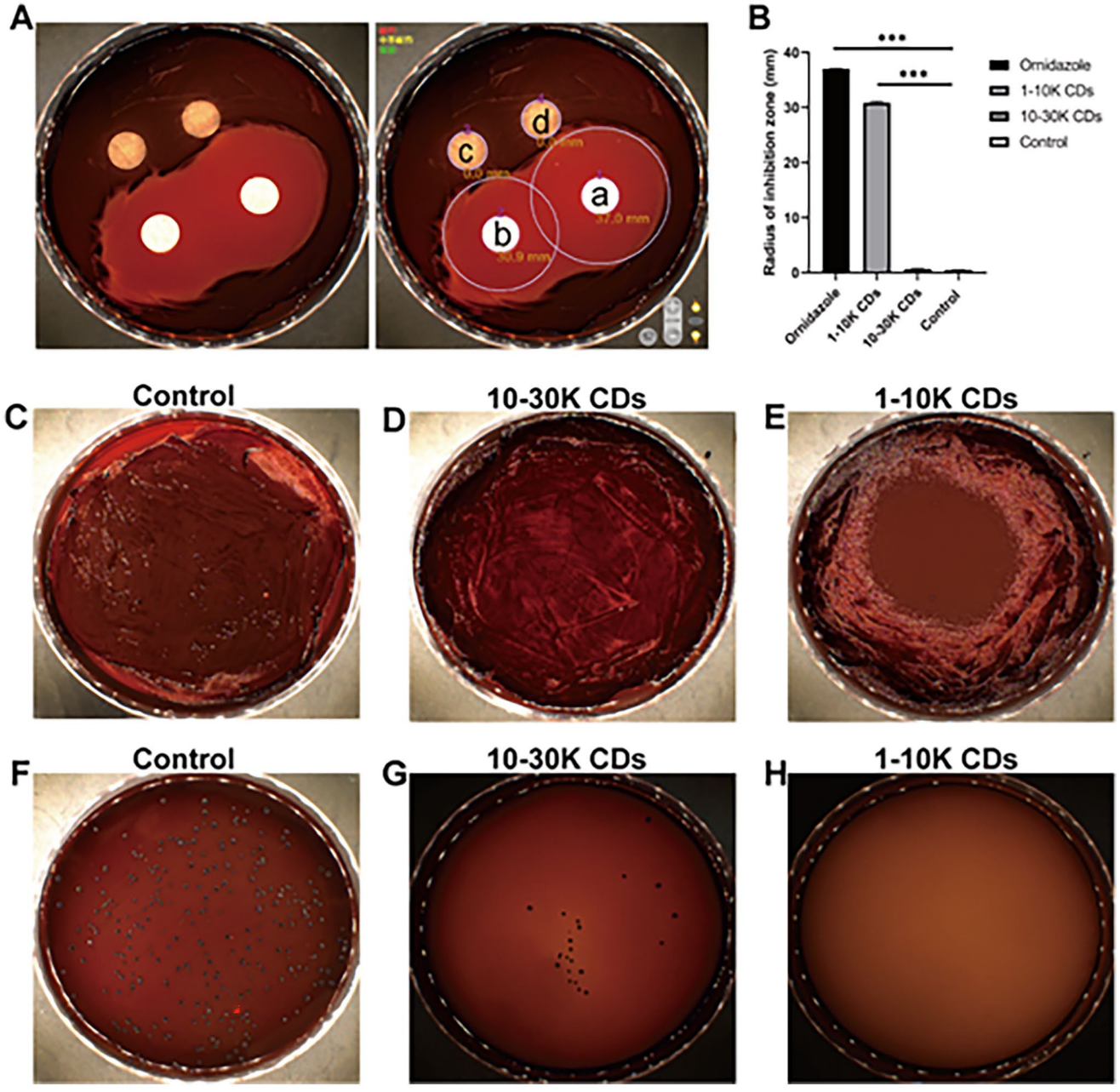

Figure 8. Inhibition experiments of *P. gingivalis*. (A) Inhibition zone experiments of (a) 100 μg/mL ornidazole, (b)100 μg/mL 1-10K CDs, (c)100 μg/mL 10-30K CDs, and (d) Control on *P. gingivalis*. (B) Statistical results of the inhibition zone radius. Co-culture of material solution and *P. gingivalis*. (C) Control (*P. gingivalis* + BHI), (D) *P. gingivalis* + 10-30K CDs and (E) *P. gingivalis* + 1-10K CDs. (F to H) The diluted plate coating count results of (C to F). (F) Diluted of (C), (G) Diluted of (D), and (H) Diluted of (E).

stronger the bactericidal effect. Once more than this critical value, there is no antibacterial effect. Hence, 1-10K CDs with smaller molecular weights exhibited significant antibacterial effects. However, both the 1-10K CDs and 10-30K CDs were not sensitive to *S. mutans*. Ornidazole contains nitro groups in the molecule and is mainly an anti-anaerobic-bacteria drug. Nitro groups are reduced to amino groups in an anaerobic environment or interact with cellular components through free radical formation, leading to microbial death. CDs retain their original nitro groups, thereby exerting certain antibacterial effects;[13] the nitro group is mainly resistant to anaerobic bacteria, such as *P. gingivalis*, while the variable chain belongs to microaerobic bacteria. Therefore, CDs had selective antibacterial effects on *P. gingivalis* and were not sensitive to *S. mutans*. To sum up, this study illustrated that our newly synthesized 1-10K ornidazole CDs were selectively antibacterial on *P. gingivalis*, provided a new strategy for the treatment of diseases related to *P. gingivalis*, and further promoted the development of nano biomedicine.

Conclusions

In summary, the photoluminescent CDs were successfully prepared with the pro-drugs ornidazole through the microwave irradiation method and screened out specific-sized

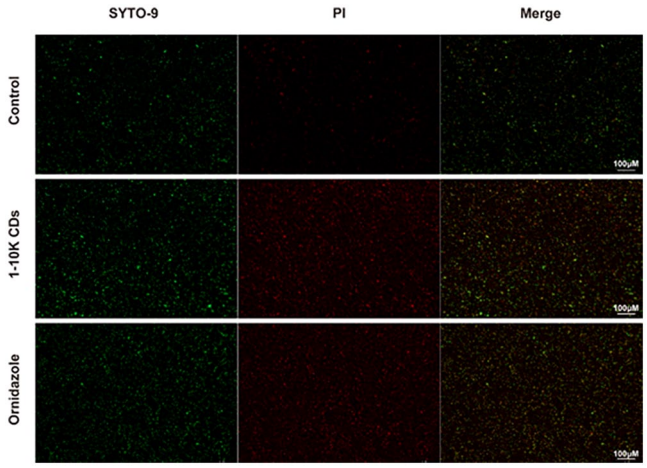

Figure 9. Typical fluorescent images of live/dead assays for the *P. gingivalis*.

CDs with fluorescence and bacteriostatic properties. The novel CDs owned low toxicity, retained excellent water solubility, and had exceedingly good bactericidal function, selectively against *P. gingivalis*. Owing to their significantly stable fluorescence, low toxicity, and dependent light emission, the hydrophilic CDs could be applied in multicolor biological imaging. In conclusion, the preparation and development of the novel CDs may be a promising way to produce nanobacteriostatic agents and provide new treatment strategy for *P. gingivalis*-related systemic diseases, as well as probe into the mechanism of diseases caused by *P. gingivalis* through real-time tracking.

AUTHORS' CONTRIBUTIONS

All authors were involved in the design of the research and data analyses and review of the manuscript; JW and YW conducted the studies and prepared the main figures, HZ and WWZ provided key reagents, JW and YW wrote the manuscript, and LKL guided the experiment.

ACKNOWLEDGEMENTS

The authors acknowledge Mingming Li for the guidance on material related analysis. The authors acknowledge Ziji Ling and Zesheng Song for the support for cell experiments and related technologies.

DECLARATION OF CONFLICTING INTERESTS

The author(s) declared no potential conflicts of interest with respect to the research, authorship, and/or publication of this article.

FUNDING

The author(s) disclosed receipt of the following financial support for the research, authorship, and/or publication of this article: This work was supported by a grant from the National Natural Science Foundation of China (NSFC, no. 81972536), Key Project of Health Commission of Jiangsu Province (no. K2019013), the Natural Science Foundation of Jiangsu Higher Education Institutions of China (no. 20KJA320003), A Project Funded by the Priority Academic Program Development of Jiangsu Higher Education Institutions (PAPD, 2018-87), and Postgraduate Research & Practice Innovation Program of Jiangsu Province (KYCX20_1409).

ORCID ID

Laikui Liu https://orcid.org/0000-0002-6509-922X

SUPPLEMENTAL MATERIAL

Supplemental material for this article is available online.

REFERENCES

1. Herrera D, Sanz M, Kebschull M, Jepsen S, Sculean A, Berglundh T, Papapanou PN, Chapple I, Tonetti MS, on behalf of the EFP Workshop Participants and Methodological Consultant. Treatment of stage IV periodontitis: the EFP S3 level clinical practice guideline. *J Clin Periodontol* 2022;**49**:4–71
2. Mysak J, Podzimek S, Sommerova P, Lyuya-Mi Y, Bartova J, Janatova T, Prochazkova J, Duskova J. Porphyromonas gingivalis: major periodontopathic pathogen overview. *J Immunol Res* 2014;**2014**:476068
3. How KY, Song KP, Chan KG. Porphyromonas gingivalis: an overview of periodontopathic pathogen below the gum line. *Front Microbiol* 2016;**7**:53
4. Singh S, Meador WE, Pramanik A, Ray P, Delcamp JH, Zhao Y. An indolizine squaraine-based water-soluble NIR dye for fluorescence imaging of multidrug-resistant bacteria and antibacterial/antibiofilm activity using the photothermal effect. *J Photochem Photobiol B* 2023;**240**:112652
5. Liang G, Wang H, Shi H, Zhu M, An J, Qi Y, Du J, Li Y, Gao S. Porphyromonas gingivalis promotes the proliferation and migration of esophageal squamous cell carcinoma through the miR-194/GRHL3/PTEN/Akt axis. *ACS Infect Dis* 2020;**6**:871–81
6. Bae K, Zheng W, Ma Y, Huang Z. Real-time monitoring of pharmacokinetics of antibiotics in biofilms with Raman-tagged hyperspectral stimulated Raman scattering microscopy. *Theranostics* 2019;**9**:1348–57
7. Dominy SS, Lynch C, Ermini F, Benedyk M, Marczyk A, Konradi A, Nguyen M, Haditsch U, Raha D, Griffin C, Holsinger LJ, Arastu-Kapur S, Kaba S, Lee A, Ryder MI, Potempa B, Mydel P, Hellvard A, Adamowicz K, Hasturk H, Walker GD, Reynolds EC, Faull RLM, Curtis MA, Dragunow M, Potempa J. Porphyromonas gingivalis in Alzheimer's disease brains: evidence for disease causation and treatment with small-molecule inhibitors. *Sci Adv* 2019;**5**:eaau3333
8. Cruz DFD, Duarte PM, Figueiredo LC, da Silva HDP, Retamal-Valdes B, Feres M, Miranda TS. Metronidazole and amoxicillin for patients with periodontitis and diabetes mellitus: 5-year secondary analysis of a randomized controlled trial. *J Periodontol* 2021;**92**:479–87
9. Alauzet C, Lozniewski A, Marchandin H. Metronidazole resistance and nim genes in anaerobes: a review. *Anaerobe* 2019;**55**:40–53
10. Ngobese B, Singh R, Han KSS, Tinarwo P, Mabaso N, Abbai NS. Detection of metronidazole resistance in Trichomonas vaginalis using uncultured vaginal swabs. *Parasitol Res* 2022;**121**:2421–32
11. Ciulla MG, Gelain F. Structure-activity relationships of antibacterial peptides. *Microb Biotechnol* 2023;**16**:757–77
12. Liu J, Li D, Zhang K, Yang M, Sun H, Yang B. One-step hydrothermal synthesis of nitrogen-doped conjugated carbonized polymer dots with 31% efficient red emission for in vivo imaging. *Small* 2018;**14**:e1703919
13. Liu J, Lu S, Tang Q, Zhang K, Yu W, Sun H, Yang B. One-step hydrothermal synthesis of photoluminescent carbon nanodots with selective antibacterial activity against Porphyromonas gingivalis. *Nanoscale* 2017;**9**:7135–42
14. Ruan S, Qian J, Shen S, Zhu J, Jiang X, He Q, Gao H. A simple one-step method to prepare fluorescent carbon dots and their potential application in non-invasive glioma imaging. *Nanoscale* 2014;**6**:10040–7
15. Rode A, Sharma S, Mishra DK. Carbon nanotubes: classification, method of preparation and pharmaceutical application. *Curr Drug Deliv* 2018;**15**:620–9
16. Lu S, Xue M, Tao A, Weng Y, Yao B, Weng W, Lin X. Facile microwave-assisted synthesis of functionalized carbon nitride quantum dots as fluorescence probe for fast and highly selective detection of 2,4,6-trinitrophenol. *J Fluoresc* 2021;**31**:19

17. Yao L, Zhao MM, Luo QW, Zhang YC, Liu TT, Yang Z, Liao M, Tu P, Zeng KW. Carbon quantum dots-based nanozyme from coffee induces cancer cell ferroptosis to activate antitumor immunity. *ACS Nano* 2022;**16**:9228–39
18. Shahba H, Sabet M. Two-step and green synthesis of highly fluorescent carbon quantum dots and carbon nanofibers from pine fruit. *J Fluoresc* 2020;**30**:927–38
19. Liao H, Ran Y, Zhong J, Li J, Li M, Yang H. Panax notoginseng powder-assisted preparation of carbon-quantum-dots/BiOCl with enriched oxygen vacancies and boosted photocatalytic performance. *Environ Res* 2022;**215**:114366
20. Zhang JH, Niu A, Li J, Fu JW, Xu Q, Pei DS. In vivo characterization of hair and skin derived carbon quantum dots with high quantum yield as long-term bioprobes in zebrafish. *Sci Rep* 2016;**6**:37860
21. Li YJ, Harroun SG, Su YC, Huang CF, Unnikrishnan B, Lin HJ, Lin CH, Huang CC. Synthesis of self-assembled spermidine-carbon quantum dots effective against multidrug-resistant bacteria. *Adv Healthc Mater* 2016;**5**:2545–54
22. Wang H, Song Z, Gu J, Li S, Wu Y, Han H. Nitrogen-doped carbon quantum dots for preventing biofilm formation and eradicating drug-resistant bacteria infection. *ACS Biomater Sci Eng* 2019;**5**:4739–49
23. Li P, Liu S, Cao W, Zhang G, Yang X, Gong X, Xing X. Low-toxicity carbon quantum dots derived from gentamicin sulfate to combat antibiotic resistance and eradicate mature biofilms. *Chem Commun (Camb)* 2020;**56**:2316–9
24. Otis G, Bhattacharya S, Malka O, Kolusheva S, Bolel P, Porgador A, Jelinek R. Selective labeling and growth inhibition of pseudomonas aeruginosa by aminoguanidine carbon dots. *ACS Infect Dis* 2019;**5**: 292–302
25. Shaikh AF, Tamboli MS, Patil RH, Bhan A, Ambekar JD, Kale BB. Bio-inspired carbon quantum dots: an antibiofilm agents. *J Nanosci Nanotechnol* 2019;**19**:2339–45
26. Hill SA, Benito-Alifonso D, Davis SA, Morgan DJ, Berry M, Galan MC. Practical three-minute synthesis of acid-coated fluorescent carbon dots with tuneable core structure. *Sci Rep* 2018;**8**:12234
27. Hajishengallis G. Immunomicrobial pathogenesis of periodontitis: keystones, pathobionts, and host response. *Trends Immunol* 2014;**35**: 3–11
28. Liang G, Shi H, Qi Y, Li J, Jing A, Liu Q, Feng W, Li G, Gao S. Specific anti-biofilm activity of carbon quantum dots by destroying ***P. gingivalis*** biofilm related genes. *Int J Nanomedicine* 2020;**15**:5473–89
29. Architha N, Ragupathi M, Shobana C, Selvankumar T, Kumar P, Lee YS, Kalai SR. Microwave-assisted green synthesis of fluorescent carbon quantum dots from Mexican Mint extract for Fe(3+) detection and bio-imaging applications. *Environ Res* 2021;**199**:111263
30. Che Y, Pang H, Li H, Yang L, Fu X, Liu S, Ding L, Hou J. Microwave-assisted fabrication of copper-functionalized carbon quantum dots for sensitive detection of histidine. *Talanta* 2019;**196**:442–8
31. Yuan JM, Zhao R, Wu ZJ, Li W, Yang XG. Graphene oxide quantum dots exfoliated from carbon fibers by microwave irradiation: two photoluminescence centers and self-assembly behavior. *Small* 2018;**14**:e1703714
32. Fung HB, Doan TL. Tinidazole: a nitroimidazole antiprotozoal agent. *Clin Ther* 2005;**27**:1859–84
33. Ingham HR, Hall CJ, Sisson PR, Tharagonnet D, Selkon JB. The activity of metronidazole against facultatively anaerobic bacteria. *J Antimicrob Chemother* 1980;**6**:343–7
34. Munir MU, Ahmad MM. Nanomaterials aiming to tackle antibiotic-resistant bacteria. *Pharmaceutics* 2022;**14**:582
35. Zheng L, Li J, Yu M, Jia W, Duan S, Cao D, Ding X, Yu B, Zhang X, Xu FJ. Molecular sizes and antibacterial performance relationships of flexible ionic liquid derivatives. *J Am Chem Soc* 2020;**142**:20257–69

(Received April 18, 2023, Accepted September 11, 2023)